Study of NH Stretching Vibrations in Small Ammonia Clusters by Infrared Spectroscopy in He Droplets and ab Initio Calculations†

Mikhail N. Slipchenko,‡ Boris G. Sartakov,§ and Andrey F. Vilesov*

Department of Chemistry, University of Southern California, Los Angeles, California 90089

Sotiris S. Xantheas

Chemical & Materials Sciences Division, Pacific Northwest National Laboratory, 902 Battelle Boulevard, P. O. Box 999, MS K1-83, Richland, Washington 99352

Received: February 14, 2007; In Final Form: March 29, 2007

Infrared spectra of the NH stretching vibrations of $(NH_3)_n$ clusters ($n = 2-4$) have been obtained using the helium droplet isolation technique and first principles electronic structure anharmonic calculations. The measured spectra exhibit well-resolved bands, which have been assigned to the ν_1, ν_3, and $2\nu_4$ modes of the ammonia fragments in the clusters. The formation of a hydrogen bond in ammonia dimers leads to an increase of the infrared intensity by about a factor of 4. In the larger clusters the infrared intensity per hydrogen bond is close to that found in dimers and approaches the value in the NH_3 crystal. The intensity of the $2\nu_4$ overtone band in the trimer and tetramer increases by a factor of 10 relative to that in the monomer and dimer, and is comparable to the intensity of the ν_1 and ν_3 fundamental bands in larger clusters. This indicates the onset of the strong anharmonic coupling of the $2\nu_4$ and ν_1 modes in larger clusters. The experimental assignments are compared to the ones obtained from first principles electronic structure anharmonic calculations for the dimer and trimer clusters. The anharmonic calculations were performed at the Møller−Plesset (MP2) level of electronic structure theory and were based on a second-order perturbative evaluation of rovibrational parameters and their effects on the vibrational spectra and average structures. In general, there is excellent (<20 cm^{-1}) agreement between the experimentally measured band origins for the N−H stretching frequencies and the calculated anharmonic vibrational frequencies. However, the calculations were found to overestimate the infrared intensities in clusters by about a factor of 4.

I. Introduction

NH_3, H_2O, and HF are fundamental examples of hydrogen-bonded (HB) systems, which differ considerably in HB strength, HB coordination, and electronic structure of the constituent molecules. An ammonia molecule has a single lone-pair orbital and three hydrogen atoms to donate, and is known to be a weak donor. Ammonia dimers exemplify a weak ($\Delta E_e \approx 3$ kcal/mol), nonlinear hydrogen bond (see ref 1 and references therein). The structure of crystalline ammonia shows that each molecule is a triple donor and an acceptor for three other protons, which share the same lone-pair orbital of nitrogen atoms.[2] In comparison, water molecules serve as double donors and double acceptors, according to the number of hydrogen atoms and lone-pair electron orbitals of the oxygen atoms. Water dimers exemplify a stronger ($\Delta E_e \approx 5$ kcal/mol), almost linear hydrogen bond.[3,4] The structures of water clusters, liquid water, and ice are mainly determined by the nearly tetrahedral arrangement of the H atoms and lone pairs in the H_2O molecules. These analogies and differences stimulated a lot of interest in ammonia clusters. In comparison to water clusters, there are relatively few studies of ammonia clusters.

Gas-phase ammonia molecules have been studied extensively by microwave, infrared, and Raman spectroscopies.[5−14] Ammonia dimers have been obtained in free jet and studied by microwave and far-infrared spectroscopies, as well as by double resonance spectroscopy.[15−24] From the high-resolution rotational spectra several structural parameters of the dimer were obtained as follows: intermolecular distance $R = 3.366$ Å; orientations of the axes of the molecules with respect to the intermolecular axis $\Theta_1 = 48.6°$ and $\Theta_2 = 115.5°$, respectively. Thus the structure of the dimer deviates considerably from that expected for a linear HB system. This unexpected structure and low binding energy of the dimer even initiated questions of whether a hydrogen bond exists at all.[23] It was later shown that the ammonia molecules in the dimer participate in the large amplitude interchange tunneling motion. Analysis of the spectra and numerical simulations allowed the reconstruction of the potential energy surface of the dimer.[25−28] The intermolecular potential was found to have an equilibrium hydrogen-bonded structure close to linear with $\Theta_1 = 32.0°$, $180° - \Theta_2 = 91.5°$, but has a low potential barrier for interchange tunneling motion of about 24 cm^{-1}.

The structure of the small ammonia clusters has also been studied from first principles electronic structure calculations.[1,29−34] The calculated hydrogen bond in dimers was consistently found to be close to linear. Ammonia trimer and tetramer clusters were found to have cyclic structures.[1,29,30,32,34] Recently, the ν_1 and ν_3 vibrations of NH_3 clusters have been studied using a

† Part of the "Roger E. Miller Memorial Issue".

‡ Present address: 1605 Gilman Hall, Department of Chemistry, Iowa State University, Ames, IA 50011-3111.

§ On leave from: General Physics Institute, Russian Academy of Sciences, Moscow, 119991, Russia.

10.1021/jp071279+ CCC: $37.00
Published on Web 05/27/2007

molecular perturbation approach in conjunction with an empirical pair potential.[35] The calculations predict splitting of the doubly degenerate ν_3 vibration in dimers and trimers by about 75−100 cm^{-1}, a large shift of the ν_1 band by about 50−75 cm^{-1}, and a factor of about 20 larger intensity of the ν_3 band compared with the ν_1 band. Earlier ab initio calculations[36] predicted a factor of about 80 enhancement in the intensity of the ν_3 and ν_1 bands in cyclic ammonia dimer. Nonadditive effects in ammonia trimers[34] were found to be less important as compared to water clusters.[37−39] A recent ab initio study[1] of the structure, energetics, and harmonic vibrational spectra of small ammonia clusters up to pentamers produced results that are complementary to the ones of the present study.

The spectra of the ν_2 umbrella mode of free ammonia clusters have been studied in the 10 μm range[18] using the double resonance IR−FIR technique. The dissociation of clusters upon infrared excitation with the CO_2 laser was used in order to obtain spectra of the ν_2 mode in ammonia clusters.[40−43] It was found that the inversion splitting in ammonia dimer is partially quenched and amounts to 3.7 cm^{-1} in the ν_2 excited state as compared to 35.7 cm^{-1} in NH_3 molecules. In ref 42 the deflection by a secondary He beam was used to disperse the cluster beam, and to measure the spectra of size selected ammonia clusters. The spectrum of the dimer was found to have two distinct peaks at 976.9 and 1003.4 cm^{-1}, which were assigned to excitation of two nonequivalent NH_3 molecules in the dimer. The spectrum of the trimer was found to have one single peak centered at 1016.3 cm^{-1}, which is consistent with a cyclic structure. Spectra of the ν_2 mode of NH_3 dimers in He droplets indicate quenching of the interchange tunneling splitting in helium.[44] Experiments on deflection of the beams of small ammonia clusters in the inhomogeneous electric field[45] revealed that ammonia clusters larger than dimers are nonpolar, consistent with the cyclic structures of trimers and tetramers.

The frequency and infrared intensity of the hydrogen bond bridge stretching vibration are especially sensitive to the strength and coordination of the bonding in clusters. The infrared spectrum of single ammonia molecules[14] in the N−H stretching range has two fundamental bands: the $\nu_1(A_1)$ symmetric stretch and the ν_3(E) asymmetric stretch. Two other weak bands correspond to the overtone of the asymmetric bend: $2\nu_4(A_1,l=0)$ and $2\nu_4(E,l=2)$. The infrared absorption spectra of ammonia dimers trapped in cryogenic matrixes show three pronounced bands[46,47] which have relatively small shifts of about or less than 50 cm^{-1} from the corresponding bands in single ammonia molecules. Comparison of the integrated absorptivity in the N−H stretching range of the freshly deposited matrixes with those after annealing shows the enhancement of absorption in clusters by a factor of >3.3.[46] A more recent study of the ammonia clusters in noble gas matrixes[47] revealed that the intensity ratio of the N−H stretching modes and the umbrella bending mode in dimers is a factor of about 5 larger than in single ammonia molecules. The observed enhancement was ascribed to the formation of the hydrogen bonds in clusters. However, the broadening of the spectra and complicated kinetics of the cluster formation in matrixes did not allow obtaining the infrared intensities for specific cluster sizes. Surprisingly, only a few studies of the N−H stretching bands in gas-phase ammonia clusters are available. The infrared spectra of the large ammonia clusters ($n \geq 8$) in the N−H stretching region have previously been studied in supersonic beams[48] and via slit jet expansion technique.[49] Raman spectra of ammonia clusters having about 5−50 molecules in seeded supersonic beams have also been reported.[50] The spectra in this size range do not allow resolution of specific cluster sizes and show broad ($\delta\nu \approx 50$ cm^{-1}) bands, which have been assigned to ν_1, ν_3, and $2\nu_4$ bands of ammonia molecules in clusters.

In this paper we report the results of a joint experimental and theoretical study of the hydrogen bonding as manifested by the N−H stretching vibrations in small ammonia clusters. Some preliminary results using the same technique have been published earlier,[51] while the spectra of larger clusters of up to $n = 900$ will be reported elsewhere.[52] In this work, ammonia clusters up to the tetramer have been formed in helium droplets[53−55] and their infrared absorption spectra have been measured in the range of the N−H stretches of the NH_3 molecules (3200−3500 cm^{-1}). With the aid of the theoretical calculations the ν_1, ν_3, and $2\nu_4$ bands of clusters have been identified, and their frequencies and infrared intensities have been obtained. For the dimer and trimer clusters, weak bands having small shifts with respect to the band origins of the corresponding bands in single molecules have been assigned to free N−H stretches of the NH_3 molecules. Other bands, which have larger spectral shifts and a factor of about 4 larger infrared intensities, have been assigned to the modes having large amplitudes of vibrations along the hydrogen bond. For the trimer and tetramer clusters the additional infrared intensity due to formation of the hydrogen bonds is shared between the stretching ν_1 and ν_3 and bending $2\nu_4$ bands. The experimental assignments are compared to the ones obtained by first principles electronic structure anharmonic calculations for the dimers and trimers and harmonic calculations for the tetramers. We also report average structure and rotational constants for the dimer and trimer clusters.

II. Approach

A. Experimental Details. Clusters of ammonia molecules were prepared by sequential pickup of single molecules by helium droplets and studied via infrared laser depletion spectroscopy.[53−57] Helium droplets having an average size of about 3500 atoms have been obtained upon expansion of ^{4}He gas through a 5 μm nozzle at a source pressure of $P_0 = 20$ bar at a temperature of $T_0 = 16$ K. The resulting droplet beam is passed through a 5 cm long, differentially pumped, scattering chamber, which was filled with ammonia gas at known pressure. Due to the fluid state of the helium droplets, molecules captured in sequence are free to move inside the droplet and within a short time coagulate to form a cluster, which cools rapidly to the ambient temperature of the droplets of $T = 0.38$ K.[58]

The infrared pulsed laser beam obtained from the optical parametric oscillator−amplifier (Laser Vision, spectral width 0.3 cm^{-1}, pulse duration 7 ns, pulse energy 1 mJ, repetition rate 20 Hz) was aligned antiparallel to the He droplet beam. The absorption of a laser photon by encapsulated species is followed by rapid energy transfer to the host droplets and subsequent evaporation of He atoms. The total flux of the He droplet beam is detected by a quadrupole mass filter, which is adjusted to transmit all masses larger than $M = 6$ u. The mass spectrometer was equipped with an electron beam ionizer and was installed about 80 cm downstream from the source of the droplet beam. The absorption leads to a transient decrease of the mass spectrometer signal, which is recorded by a fast digitizer. Linear dependence of the depletion signal with respect to laser pulse energy has been carefully checked. To calibrate the laser frequency, a photoacoustic cell filled with ammonia gas is used. During the experiment the mass spectrometer signal, the photoacoustic cell signal, and the laser pulse energy are measured simultaneously.

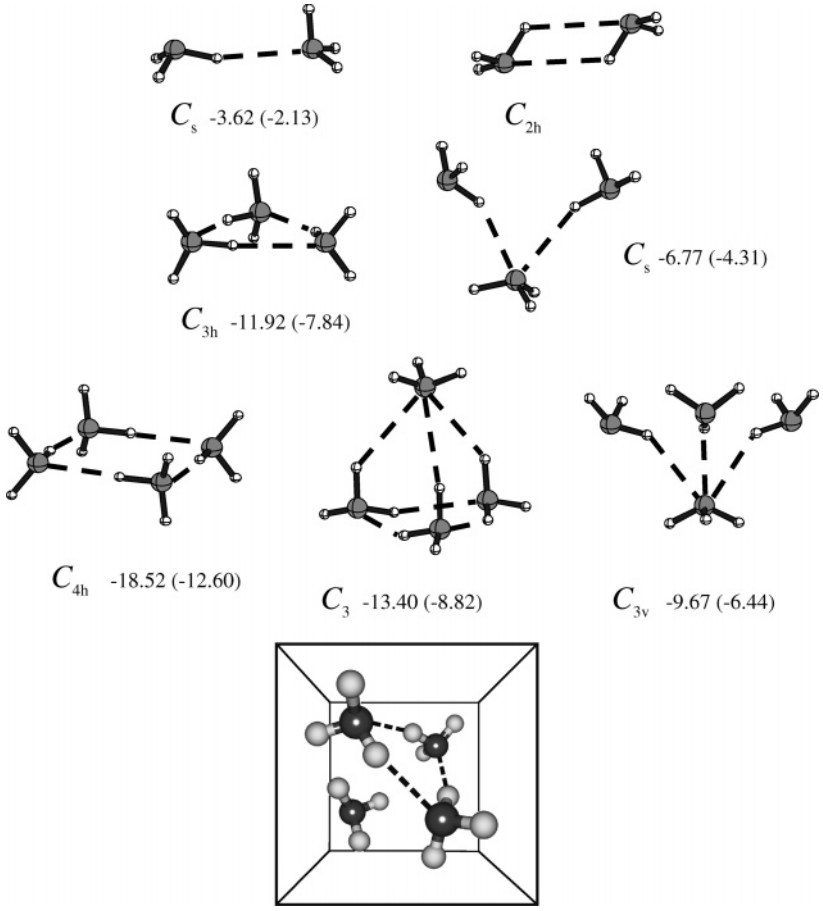

Figure 1. Calculated structures of ammonia clusters. The numbers denote the binding energies (ΔE_e) in kcal/mol computed at the MP2/aug-cc-pVDZ level with respect to *n* gas-phase monomers. Zero-point corrected binding energies (ΔE_0) are shown in parentheses. The lower picture shows the unit cell of the crystalline ammonia obtained with neutron scattering measurements adopted from ref 2.

B. Computational Details. The geometries of the monomer through tetramer clusters were optimized at the second-order Møller−Plesset (MP2) perturbation level of theory with the aug-cc-pVDZ and aug-cc-pVTZ basis sets.[59,60] For the trimer and tetramer clusters, several isomers were investigated to ensure adequate sampling of the potential energy surface and to be able to identify the global minimum. It should be noted that our approach is similar to the one used in a recent study[1] and it does, in principle, yield the same global and low-lying local minima. However, we intended to investigate higher lying networks corresponding to different arrangements and therefore different IR fingerprints in order to compare with the experimentally measured frequencies and identify the possibility of their formation. To this end we did not investigate the "tail" (or "3 + 1") arrangement of the tetramer (vide infra) as its vibrational spectrum is already reported.[1] The harmonic vibrational frequencies were computed analytically at the MP2 level of theory with the aug-cc-pVDZ (for $n = 1-4$) and aug-cc-pVTZ (for $n = 1-3$) basis sets. Anharmonic calculations were performed at the second-order perturbation theory,[61−66] which provides closed expressions for most of the spectroscopic constants needed for obtaining anharmonic frequencies. Starting from the analytical second derivatives of the electronic energy at the MP2/aug-cc-pVDZ level of theory with respect to the nuclear coordinates, the third and semidiagonal fourth derivatives were obtained by a finite difference approach for the monomer through trimer clusters following the approach suggested by Barone and co-workers.[67−69] A recent review[70] offers a critical comparison between this approach and grid-based methods for the calculation of the anharmonic frequencies of hydrogen-bonded systems. The calculations were carried out using the Gaussian 03 suites of electronic structure software[71,72] at the National Energy Research Scientific Computing Center (NERSC) at Lawrence Berkeley National Laboratory.

III. Results

A. Minimum Energy and Vibrationally Averaged Structures and Vibrational Frequencies. The minimum energy structures for the ammonia dimer through tetramer clusters are shown in Figure 1. For the trimer and tetramer several low-lying local minima are also shown. The different bonding arrangements for the $n = 3$ and 4 clusters were investigated in order to ensure adequate sampling of the potential energy surface and location of the global minimum. The total (E_e in au) and binding (ΔE_e in kcal/mol) energies of the global and local minima at the MP2 level of theory with the aug-cc-pVDZ and aug-cc-pVTZ basis sets are listed in Table A1, where zero-point corrected binding energies (ΔE_0 in kcal/mol) are also shown in parentheses. The cluster binding energies are also indicated in Figure 1, with the ones including zero-point corrections (ΔE_0) denoted in parentheses. The results of our calculations are quite similar to those obtained recently.[1] The minimum energy structure of the ammonia dimer has one hydrogen bond and C_s symmetry. The doubly hydrogen bonded (cyclic) configuration of C_{2h} symmetry is a first-order transition state. The trimer minimum energy structure corresponds to a cyclic homodromic HB network of C_{3h} symmetry having three hydrogen bonds, a structure reminiscent of the water trimer minimum.[37] A local trimer minimum of C_s symmetry having only two hydrogen

TABLE 1: Harmonic (ω) and Anharmonic (ν) Frequencies (in cm^{-1}) and IR Intensities (in km/mol) for the Ammonia Clusters $n = 2-4$ at the MP2/aug-cc-pVDZ Level of Theory

$(NH_3)_2$, C_s			$(NH_3)_3$, C_{3h}			$(NH_3)_4$, C_{4h}	
harmonic	intensity	anharmonic	harmonic	intensity[a]	anharmonic	harmonic	intensity[a]
47 (A″)	8.5	−21	125 (E″)	0.0	111	7 (B_u)	0.0
92 (A′)	65.6	45	133 (A″)	42.4	123	57 (B_g)	0.0
111 (A″)	41.5	82	145 (E′)	9.1	125	141 (E_g)	0.0
148 (A′)	27.3	119	177 (A′)	0.0	153	146 (A_u)	62.8
248 (A″)	41.7	220	248 (E″)	0.0	198	152 (A_g)	0.0
398 (A′)	46.7	326	326 (A″)	82.2	266	167 (B_u)	0.0
1072 (A′)	166.4	986	358 (E′)	128.4	292	169 (E_u)	18.1
1083 (A′)	88.4	1005	550 (A′)	0.0	493	171 (B_g)	0.0
1641 (A′)	12.1	1602	1111 (E′)	191.8	1031	259 (B_u)	0.0
1650 (A″)	15.0	1607	1144 (A′)	0.0	1054	307 (E_g)	0.0
1654 (A′)	9.8	1608	1639 (E′)	8.8	1581	335 (B_g)	0.0
1673 (A″)	6.4	1618	1664 (A′)	0.0	1615	356 (A_u)	96.0
3447 (A′)	70.7	3310	1677 (E″)	0.0	1626	449 (E_u)	114.9
3476 (A′)	4.2	3318	1678 (A″)	21.6	1630	560 (A_g)	0.0
3597 (A′)	67.8	3435	3404 (A′)	0.0	3291	1136 (B_g)	0.0
3628 (A′)	8.4	3451	3421 (E′)	165.2	3293	1145 (E_u)	222.9
3631 (A″)	0.3	3455	3574 (A′)	0.0	3405	1166 (A_g)	0.0
3632 (A″)	9.2	3454	3578 (E′)	94.3	3406	1634 (B_g)	0.0
			3628 (E″)	0.0	3448	1645 (E_u)	15.6
			3629 (A″)	12.7	3448	1662 (A_g)	0.0
						1678 (A_u)	27.4
						1683 (E_g)	0.0
						1692 (B_u)	0.0
						3365 (Ag)	0.0
						3384 (E_u)	415.0
						3394 (B_g)	0.0
						3559 (A_g)	0.0
						3562 (E_u)	139.3
						3563 (B_g)	0.0
						3623 (B_u)	0.0
						3624 (E_g)	0.0
						3624 (A_u)	13.3

[a] In the case of the doubly degenerate E, modes the infrared intensity is given per degree of freedom. To obtain the total infrared intensities of the doubly degenerate bands, these numbers are to be multiplied by a factor of 2.

TABLE 2: Calculated Zero-Point Energies and Rotational Constants for the Ammonia Clusters at the MP2/aug-cc-pVDZ Level of Theory

	$(NH_3)_2$	$(NH_3)_3$	$(NH_3)_4$
A_e, cm^{-1}	3.986 596	0.176 074	0.090 695
B_e, cm^{-1}	0.173 453	0.176 074	0.090 695
C_e, cm^{-1}	0.171 459	0.091 884	0.004 669
A_0, cm^{-1}	4.130 478	0.172 296	
B_0, cm^{-1}	0.170 286	0.172 296	
C_0, cm^{-1}	0.168 415	0.089 448	
D_J, cm^{-1}	$0.119\,151 \times 10^{-5}$	$0.808\,322 \times 10^{-6}$	
D_{JK}, cm^{-1}	$0.634\,669 \times 10^{-4}$	$-0.125\,009 \times 10^{-5}$	
D_K, cm^{-1}	$0.679\,354 \times 10^{-3}$	$0.538\,115 \times 10^{-6}$	
ZPE(harmonic), cm^{-1}	15 615.3	24 069.0	32 259.4
ZPE(fundamental), cm^{-1}	14 810.5	22 851.3	
ZPE(anharmonic), cm^{-1}	15 212.9	23 578.6	

bonds lies 5.15 kcal/mol higher in energy (cf. Table A1 and Figure 1) from the global ring trimer minimum. This "open" trimer structure is also reminiscent of the local water trimer (d−aa−d) minimum, which also has two hydrogen bonds and a central molecule acting as a double acceptor (aa) to the two end donor (d) molecules.[73,74] The global minimum for the ammonia tetramer also corresponds to a ring homodromic structure of C_{4h} symmetry, similar to the bonding arrangement found in the water tetramer.[75] Two local minima of C_3 and C_{3v} symmetry, in which the fragment center of masses are in tetrahedral arrangements, are local minima lying 3.78 (C_3) and 6.16 kcal/mol (C_{3v}) above the global C_{4h} minimum. (cf. Table A1 and Figure 1). In comparison, recent studies have suggested[1] a four member ring structure which is either flat or has a boat configuration with energies of about 15.5 kcal/mol similar to the global minimum of the tetramer. However, the first local minimum structure was found to have a homodromic three-member ring with a fourth molecule attached in an asymmetric position to one of the three molecules. This so-called "tail" (or "3 + 1") isomer was found to have a binding energy of 12.6 kcal/mol.

The geometric parameters of the global minima of the clusters $n = 1-4$ are listed in Table A2 for both the equilibrium and vibrationally averaged geometries. We note the contraction of the intermolecular N−N separation by 0.091 Å from the dimer (3.266 Å) to the tetramer (3.175 Å). This is about half the corresponding contraction (0.177 Å) found for the water dimer to tetramer clusters,[75] and it is consistent with the fact that the cooperative three-body term is weaker for the ammonia (11%) than for the water trimer (17%). The effect of vibrational averaging on the geometric and spectroscopic constants of gas-phase NH_3 is shown in Table A3. In that table the equilibrium

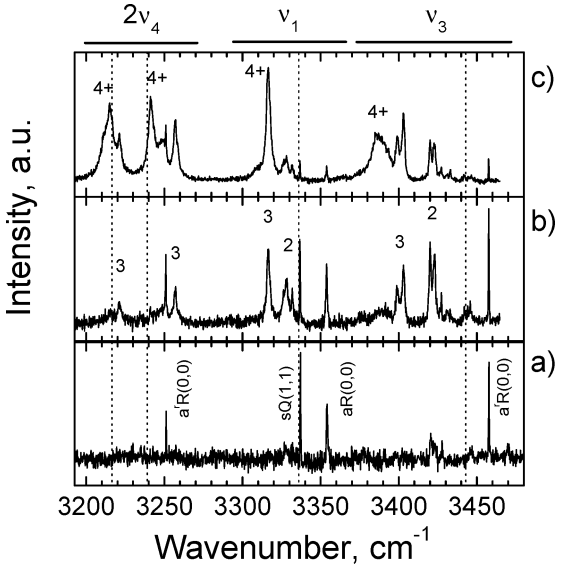

Figure 2. A series of depletion spectra normalized on the laser pulse energy as measured at increasing pickup pressure of 0.2×10^{-5}, 1.0×10^{-5}, and 3.4×10^{-5} mbar in panels a, b, and c, respectively. Panel a shows the assignment of strong rovibrational lines of single ammonia molecules.[79] Vertical dashed lines indicate the frequencies of the vibrational bands of single molecules in He droplets.[79]

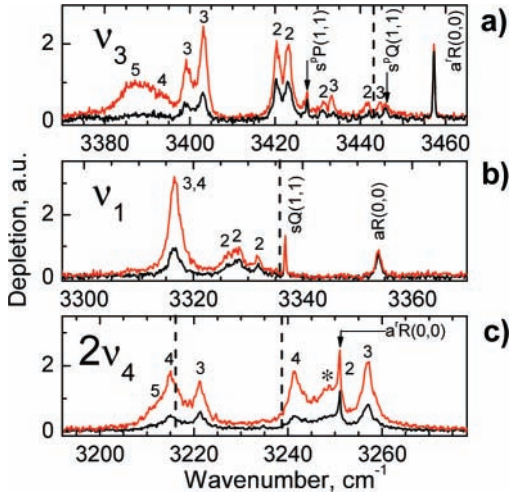

Figure 3. Depletion spectra of ammonia in He droplets in the range of the ν_3, ν_1 and $2\nu_4$ bands are shown in panels a, b, and c, respectively. Lower and upper spectra in each panel were measured at pickup pressures of 1×10^{-5} and 2×10^{-5} mbar, respectively. The assignment of strong rovibrational lines of single ammonia molecules and the assignment of the cluster bands to different cluster sizes is indicated. Due to overlap of peaks corresponding to the different cluster sizes, we were not able to assign the band indicated by (*). The origins of the corresponding bands of single ammonia molecules in He droplets are shown by dashed lines.[79]

quantities are indicated by the subscript "e" whereas the vibrationally averaged ones are indicated by the subscript "0". The effect of the basis set is also indicated by comparing the results with the aug-cc-pVDZ and aug-cc-pVTZ sets. We observe a convergence toward the experimentally obtained values[76−78] for the rotational constant and the Wilson centrifugal distortion constants D_J, D_{JK}, and D_K with increasing the basis set.

The calculated harmonic (ω) and anharmonic (ν) frequencies for the NH_3 clusters are listed in Table 1. For NH_3 the MP2/aug-cc-pVTZ anharmonic frequencies are within 40 cm^{-1} (<1%) from the experimentally observed band origins (cf. Table A3). For NH_3 the zero-point-energy correction based on the fundamentals is 5 cm^{-1} (aug-cc-pVDZ) and 50 cm^{-1} (aug-cc-pVTZ) away from the experimental value of 7214.5 cm^{-1} (cf. Table A3). As for the NH stretches, the results with the aug-cc-pVDZ basis set are fortuitously closer to the experimental band origins than the ones with the larger aug-cc-pVTZ set, although the observed differences are quite small. This finding represents a compromise between feasibility and accuracy and further justifies the use of the aug-cc-pVDZ basis set in the calculation of the anharmonic frequencies for clusters. For the harmonic frequencies, the corresponding IR intensities (in km/mol) are also given in Table 1. The cluster equilibrium and vibrationally averaged rotational constants together with the zero-point-energy corrections based on harmonic, fundamental, and anharmonic frequencies are listed in Table 2. In that table the spectroscopic constants in the symmetrically reduced Hamiltonian D_J, D_{JK}, and D_K are also listed.

B. Measured Infrared (IR) Spectra. Figure 2 shows a series of depletion spectra, which were measured at increasing pickup pressure of NH_3, $P(NH_3)$. Sharp lines in trace a, which was obtained at small $P(NH_3) = 0.2 \times 10^{-5}$ mbar, are the rovibrational transitions of the ν_1 and ν_3 fundamental bands and the $2\nu_4$ overtone band of single NH_3 molecules in He droplets.[79] At larger $P(NH_3)$ values, strong bands of ammonia dimers and trimers appear in the spectrum; see trace b. The bands of clusters are shifted by 5−60 cm^{-1} with respect to frequencies of the corresponding bands of the single molecules. Because the shift of the cluster bands is smaller than the separation of the bands in single ammonia molecules (about 100 cm^{-1}), we nominally label cluster bands as ν_1, ν_3, and $2\nu_4$ (note that our results indicate a strong interaction of the ν_1 and $2\nu_4$ modes in the ammonia trimer and tetramer clusters). The spectra for each of the vibrational bands of the clusters and the assignments of the observed spectral features are shown in Figure 3. We assign the strong bands to the vibrations of the donor bridge H-bonded stretching modes of the clusters, which have been enhanced due to formation of the hydrogen bonds. The weak peaks close to the origins of the bands of single ammonia molecules are assigned to the N−H stretches of the proton acceptor molecules in dimers and the free N−H stretches in trimers. At larger $P(NH_3)$ the bands of tetramers are shown in trace c of Figure 2. No additional spectral features appear at even larger $P(NH_3)$ values, a fact that indicates that the vibrational shift converges and the bands of larger clusters appear at approximately the same frequencies. The frequency shift of the ν_1 mode saturates at $n = 3$, so trimers and larger clusters contribute to a rather sharp band at $\nu = 3316.5$ cm^{-1}.

C. Assignment of the Cluster Bands. The assignment of the bands to particular cluster sizes has been facilitated by measurements of the pressure dependence of the intensity. Figure 4 shows the $P(NH_3)$ dependence of the intensity of the three spectral features, i.e., at $\nu = 3457$ cm^{-1} (squares), at $\nu = 3420$ cm^{-1} (circles), and at $\nu = 3403$ cm^{-1} (diamonds). At larger pressure of ammonia in the pickup cell, the broad peaks, which originate from the larger ammonia clusters (see Figure 2), contribute to the measured intensities. To eliminate this contribution from larger clusters, the background signal defined as the average of the signal measured at both sides of the studied peaks has been subtracted. It is seen that the intensities reach their maximum values at different values of $P(NH_3)$, which are approximately in the ratio of 1:2:3. This ratio is expected for the pressure dependence of monomers, dimers, and trimers, respectively. Solid curves in Figure 4 are Poisson fits of the intensity vs pickup pressure for the monomer, dimer, and trimer clusters, respectively, as will be described in the following

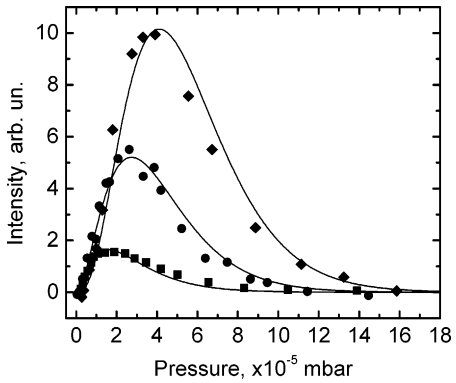

Figure 4. Dependence of the depletion signal, I_n, on the NH_3 pressure in the pickup cell, as measured for some bands in the ν_3 range (see Figure 3a): squares, $a^rR(0,0)$ line of single molecules at $\nu = 3457$ cm^{-1}; circles, dimer band at $\nu = 3420$ cm^{-1}; diamonds, trimer band at $\nu = 3403$ cm^{-1}. Each curve has been normalized on the sum of the integrated intensities of all spectral peaks in Figure 3, assigned to monomers, dimers, and trimers. Solid curves are fits according to scaled Poisson distribution for monomers, dimers and trimers, respectively; see eqs 2 and 3 in the text.

section. The good correspondence between the measurements and the fits supports the assignment of the spectral features to monomers, dimers, and trimers, respectively. Other bands were assigned based on the fact that relative intensity of the bands in the spectra shown in Figures 2 and 3, which originate from clusters of the same size, is independent of $P(NH_3)$.

Dimers. Four peaks were assigned to dimers in the ν_3 range; see Figure 3a. The two peaks at 3420.4 and 3423.1 cm^{-1} are associated with a large shift from the band origin of single molecules at 3443.1 cm^{-1} and are about a factor of 6 stronger than the two other peaks at 3431.2 and 3441.5 cm^{-1}. In the range of the ν_1 band three stronger peaks and one low-intensity peak for the dimer are identified; see Figure 3b. The low-intensity peak at 3334.7 cm^{-1} was clearly identified in the course of the study of the inversion splitting of single ammonia molecules in He droplets (see Figure 4 in ref 79). In the range of the $2\nu_4$ overtone bands only one weak peak at 3251 cm^{-1} could tentatively be assigned to the dimer. At small $P(NH_3)$ this peak is overlapping with a stronger line of single ammonia molecules at 3250.9 cm^{-1},[79] and at high $P(NH_3)$ it is overlapping with strong peaks of larger ammonia clusters. Therefore, the relative intensity of the 3251 cm^{-1} band of the dimer is expected to be accurate to within a factor of 2. The relative intensities of the spectral peaks of the cluster bands have been obtained from the fits of the spectrum by the sum of Lorentz shapes:

$$I(\omega) = y_o + \sum_k \frac{2A_k}{\pi} \frac{w_k}{4(\nu - \nu_k)^2 + w_k^2} \qquad (1)$$

where y_o is a baseline, A_k is an integral intensity, and w_k is the width (full width at half-maximum) and ν_k the origin of the kth band in the spectrum. We empirically found that the Lorentz waveform of the fits gave better representation of the spectra. For comparison, Gaussians provided better fits of the sharp lines of the monomers, whose line width is limited by the laser source. The experimentally measured and calculated frequencies and intensities of the assigned peaks of the dimer are compiled in Table 3.

Trimers. In the range of the ν_3 band four spectral features have been assigned to the trimer. Two strong close-lying peaks at 3399.2 and 3403 cm^{-1} have a spectral shift of about 40 cm^{-1} from the ν_3 band origin of single ammonia molecules. As in the case of the dimer, two weak bands close to the ν_3 band origin of single molecules have been assigned to the trimer at 3433.3 and 3444.6 cm^{-1} toward low frequency. In the ν_1 range only one intense band at 3316.5 cm^{-1} was assigned to the trimer. In the range of the $2\nu_4$ band two intense bands at 3221 and 3256.5 cm^{-1} have also been assigned to the trimer. The frequencies are close to the band origins of the two components of the $2\nu_4$ overtone of single molecules at 3216.1 cm^{-1} ($l = 0$) and at 3238.7 cm^{-1} ($l = 2$). When compared to the dimer, where we could barely identify the overtone bands, the intensity in the overtone bands in the trimer is comparable to that of the fundamental bands. The experimentally measured and calculated frequencies and intensities of the assigned peaks of the trimer are compiled in Table 4.

Tetramers. Only strong bands could be identified for the ammonia tetramer in the spectra of Figure 3. All identified bands have a considerable overlap with bands of smaller and/or larger clusters. Therefore, the parameters of the bands listed in Table 5 may be associated with considerable error. In particular, the relative intensities of the bands are estimated to be accurate to within a 50% error bar.

D. Infrared Intensities of the Cluster Bands. The He droplet may be viewed as a nanocalorimeter. Upon absorption of a photon, a number of He atoms proportional to the photon energy are evaporated. The integral of the depletion signal over the vibrational band of clusters having n molecules, I_n, is proportional to the energy of the absorbed photons, $h\nu_n$, the infrared intensity (IRI) of the cluster band, A_n, and the abundance of the clusters, $[(NH_3)_n]$:

$$I_n = C(h\nu_n)A_n[(NH_3)_n] \qquad (2)$$

where C is an amplitude factor. Following previous studies,[53,56] the abundance of the clusters having n molecules in the He droplet beam is given by the Poisson distribution:

$$[(NH_3)_n] = \frac{z^n}{n!}\exp(-z) \qquad (3)$$

where $z = \chi P(NH_3)$ is the average number of pickup events per droplet, $P(NH_3)$ is the pressure of the ammonia gas in the pickup chamber, and χ is a numerical factor. Figure 4 shows the dependence of the total intensity, I_n, of the spectral bands of the $(NH_3)_n$ ($n = 1-3$) clusters versus the ammonia pressure in the pickup chamber, $P(NH_3)$. Each experimental curve in Figure 4 has been normalized on the sum of the intensities of the observed bands of the monomers, dimers, and trimers, respectively, depicted in Figures 2 and 3. The solid curves in Figure 4 are fits of the experimental curves using eqs 2 and 3.

The ratio of the IRI of the clusters of n and $(n - 1)$ molecules, A_n/A_{n-1}, could be obtained from the corresponding intensity ratio I_n/I_{n-1}. According to eqs 2 and 3

$$\frac{I_n}{I_{n-1}} = \frac{\nu_n A_n}{\nu_{n-1} A_{n-1}} \frac{\chi P_M}{n} \qquad (4)$$

The experimental results indicate that the dependence of the ratio I_n/I_{n-1} versus P_M is sublinear at $P_M > 3 \times 10^{-5}$ mbar. We attribute this deviation to the effect of the droplet size distribution and scattering of the droplet beam at high pickup pressure. Therefore, values of A_n/A_{n-1} were obtained from the average slopes of the I_n/I_{n-1} vs P_M at $P_M \leq 2 \times 10^{-5}$ mbar. To obtain absolute values of the IRI, we used the known IRI of single molecules of $A_1 = (5.8 \pm 0.3)$ km/mol[14] for the ν_1 band of ammonia. In practice, the intensities of the well-resolved (1, 0)

TABLE 3: Band Centers, Widths, Relative Intensities, and Infrared Intensities of the $(NH_3)_2$ Bands

	ν, cm^{-1}				infrared intensity, km/mol	
band	experiment	calculation[e]	width, cm^{-1}	intensity,[c] au	experiment	calculation[e]
			ν_3 (Monomer: $\nu_3 = 3443.1$ cm^{-1}, $A = 2.9$ km/mol)[a]			
A″		3455				0.3
A″	3441.5	3454	1.8	0.17	2.5	9.2
A′	3431.2	3451	1.4	0.16	2.4	8.4
A′	3423.1	3435	1.7	1[c]	14.8 27[f]	67.8
	3420.4		1.5	0.83	12.2	
			ν_1 (Monomer: $\nu_1 = 3335.8$ cm^{-1}, $A = 5.8$ km/mol)[a]			
?	3334.7	?	0.6	0.04	0.6	
A′	3331.8	3318	1.46	0.34	5.0	4.2
A′	3328.2	3310	2.0	0.77	11.4 16.6[f]	70.7
	3326.2		1.5	0.35	5.2	
			$2\nu_4$ (Monomer, $l = 2$: $\nu = 3238.7$ cm^{-1}, $A = 0.7$ km/mol)[a]			
			$2\nu_4$ (Monomer, $l = 0$: $\nu = 3216.1$ cm^{-1}, $A = 0.05$ km/mol)[a]			
$2\nu_4$	3251	3196, 3207[d]	1.5	0.10	1.5[b]	

[a] The monomer band origins were taken from ref 79 and infrared intensities from ref 14. [b] This peak is overlapping with peaks from single ammonia molecules and larger ammonia clusters and is only tentatively assigned to ammonia dimers. [c] The areas of the spectral peaks have been normalized to that for the $\nu = 3423.1$ cm^{-1} peak. [d] Two (nondegenerate) bands at 3196 cm^{-1} and two bands at 3207 cm^{-1}, respectively. [e] Anharmonic frequencies. [f] Sum of the two components.

TABLE 4: Band Centers, Widths, Relative Intensities, and Infrared Intensities of the $(NH_3)_3$ Bands

	ν, cm^{-1}				infrared intensity, km/mol	
band	experiment	calculation[g]	width, cm^{-1}	intensity,[c] au	experiment	calculation
			ν_3 (Monomer: $\nu_3 = 3443.1$ cm^{-1}, $A = 2.9$ km/mol)[a]			
A″	3444.6	3448	1.9	0.13	3.0	12.7
E″		3448				0
?	3433.3		1.2	0.14	3.3	
E′	3403.0	3406	1.8	1[c]	22.9 39.4[h]	188[d]
	3399.2		2.5	0.72	16.5	
A′		3405				0
			ν_1 (Monomer: $\nu_1 = 3335.8$ cm^{-1}, $A = 5.8$ km/mol)[a]			
E′	3316.5	3293	2.5	1.73	39.7[b]	330[d]
A′		3291				0
			$2\nu_4$ (Monomer, $l = 2$: $\nu = 3238.7$ cm^{-1}, $A = 0.7$ km/mol)[a]			
$2\nu_4$	3321.0	3215, 3248[e]	3.5	1.59	36.4[b]	
			$2\nu_4$ (Monomer, $l = 0$: $\nu = 3216.1$ cm^{-1}, $A = 0.05$ km/mol)[a]			
$2\nu_4$	3256.5	3154, 3223[f]	3.5	0.85	19.5	

[a] The monomer band origin frequencies were taken from ref 79 and infrared intensities from ref 14. [b] This peak is overlapping with peaks of larger ammonia clusters and its intensity was deconvoluted using pressure dependence. [c] The areas of the spectral peaks have been normalized to that for the $\nu = 3403$ cm^{-1} peak. [d] Total intensity of the doubly degenerate mode. [e] Overtones of the anharmonic bands at 1626 and 1630 cm^{-1} in the trimer. [f] Overtones of the anharmonic bands at 1581 and 1615 cm^{-1} in the trimer. [g] Anharmonic frequencies. [h] Sum of the two components.

TABLE 5: Band Centers, Widths, Relative Intensities, and Infrared Intensities of the $(NH_3)_4$ Bands

	ν, cm^{-1}				infrared intensity, km/mol	
band	experiment	calculation[f]	width, cm^{-1}	intensity,[d] au	experiment	calculation
			ν_3 (Monomer: $\nu_3 = 3443.1$ cm^{-1}, $A = 2.9$ km/mol)[a]			
E_u	3392[b]	3562	7	0.38	34.8	278[e]
			ν_1 (Monomer: $\nu_1 = 3335.8$ cm^{-1}, $A = 5.8$ km/mol)[a]			
E_u	3316.5[c]	3384	2.5	0.25	22.9	830[e]
			$2\nu_4$ (Monomer, $l = 2$: $\nu = 3238.7$ cm^{-1}, $A = 0.7$ km/mol)[a]			
$2\nu_4$	3241[b]		3	0.97	88.9	
			$2\nu_4$ (Monomer, $l = 0$: $\nu = 3216.1$ cm^{-1}, $A = 0.05$ km/mol)[a]			
$2\nu_4$	3216[b]		3.5	1[d]	91.6	

[a] The monomer band origin frequencies were taken from ref 79 and infrared intensities from ref 14. [b] These tetramer peaks are overlapped with peaks of trimers and larger ammonia clusters ($n \geq 5$); see Figure 3. [c] This peak is overlapped with peaks from ammonia trimer; see Figure 3b. [d] The areas of the spectral peaks have been normalized to that for the $\nu = 3216$ cm^{-1} peak. [e] Total intensity of the doubly degenerate mode. [f] Harmonic frequencies.

← (0, 0) line of NH_3 molecules have been measured. Intensities of the few other lines of the ν_1 band, which are present at the temperature of 0.38 K[58] in the He droplet, were calculated using known line strength factors and abundance of nuclear spin isomers of NH_3. The obtained IRIs for different cluster bands are listed in Tables 3−5. The errors in the IRI values are estimated to be 20% and 30% for the dimer and trimer clusters, respectively. The intensity of the ammonia tetramers has been estimated from the deconvolution of the strongly overlapping bands; however, as noted earlier it can be associated with a 50% error bar. The accuracy of the IRI of the free N−H stretch bands is about 50% due to the low intensity of these bands. It

is believed that the IRIs obtained in this work are not greatly perturbed by encapsulation in He droplets. This conjecture is supported by the fact that the vibrational frequencies[53,55,56] and permanent dipole moments[80] of molecules in He droplets remain within about 0.01% and 1% from the corresponding values in free molecules, respectively.

IV. Discussion

Liquid helium exhibits the most gentle matrix effect due to the weak interaction of molecules with He atoms. The frequency shift of the ν_1, ν_3 bands and $2\nu_4$ bands of single ammonia molecules in He droplets were found to be in the range of -0.2 to -0.6 cm^{-1},[79] i.e., less than 0.02% from their corresponding gas-phase values. Due to the small magnitude of the matrix shift, the measured frequencies in the clusters are expected to be essentially the same as the gas-phase frequencies. Therefore, the assignment of the observed spectral bands of the clusters is based on the calculated frequencies and infrared intensities of those bands.

A. Dimers. Table 3 shows the comparison of the measured and calculated anharmonic frequencies of the ν_1 and ν_3 bands in the dimers. The calculations suggest that the ammonia dimer has a hydrogen-bonded C_s structure; see Figure 1. In the dimer each of the $\nu_1(A_1)$ and $\nu_3(E)$ bands are expected to give rise to two and four components, respectively, according to their degeneracy. The bands at 3441.5, 3431.2, and 3331.8 cm^{-1}, which have small shifts from the band origins of the ν_3 and ν_1 bands of single NH_3 molecules, are assigned to the corresponding vibrations of the acceptor molecules in agreement with the results of the normal-mode analysis. The intensities of the free N−H stretch bands are small and comparable to those in the free molecules. The strong spectral peaks at about 3422 and 3327 cm^{-1} are assigned to the ν_3 and ν_1 bands of the donor molecules, which have large amplitudes of vibrations of the hydrogen-bonded H atom. The intensities of the ν_3 and ν_1 bands are factors of about 9 and 3 larger than the corresponding bands of single ammonia molecules. The strong enhancement of the IRI is consistent with the formation of a hydrogen bond in the dimer. The effect of band enhancement is in qualitative agreement with the results of calculations although the calculated IRIs are factors of about 2.5 and 4 larger than the experimental results, respectively.

The ν_3 band has two components of similar intensity, which have a splitting of about 2.7 cm^{-1}. A natural explanation of the splitting would be the lifting of the degeneracy of the ν_3 band of the donor molecules. However, this explanation is not supported by the results of the calculations, which suggest a larger splitting of about 16 cm^{-1} for the two components of the ν_3 band of the donor molecules. The second band at 3451 cm^{-1} has a low IRI.

According to the calculations (cf. Table 2) the ammonia dimer $(NH_3)_2$ is a nearly symmetric top with rotational constants $A_0 = 4.130$ cm^{-1} and $B_0 = 0.170$ cm^{-1}. Because the direction of the N−H−N hydrogen bond is close to the inertia a-axis of the complex, we expect the enhanced bands in dimers to be close to parallel. The rotational structure due to the end-over-end rotation is not resolved at the laser line width of the present experiment of ∼0.3 cm^{-1}. Therefore, the spectrum of a rigid symmetric top with the above rotational constants at 0.38 K should contain a single band.

The splitting of the band could also arise from the inversion and interchanged splitting in ammonia dimers. The 10 μm band of ammonia dimers in He droplets[44] has four components, which have been assigned to transitions into the inversion − interchange components of the split ν_2 band of ammonia dimers. It was concluded[44] that the interchange splitting, which has a magnitude of about 20 cm^{-1} in the free ground state ammonia dimers, is quenched to less than 2 cm^{-1} in He droplets. Therefore, the observed splitting could be tentatively assigned to transitions into interchange states in the ν_3 excited state of ammonia dimers. According to this interpretation a similar splitting should be observed for the ν_1 band of the dimers. Indeed, the ν_1 band shows some splitting of about 2 cm^{-1}.

The anharmonic overtones of the ν_4 dimer fundamentals of 1602, 1607, 1608, and 1618 cm^{-1} (cf. Table 1) are calculated at 3196, 3196, 3207, and 3207 cm^{-1} (for the $2\nu_4$) as listed in Table 3. These values are within 50 cm^{-1} of the experimentally observed band origin for the ($2\nu_4$) overtone at 3251 cm^{-1}.

B. Trimers. The spectral trend observed in the dimers continues for the trimers as well; see Table 4. The global minimum of the ammonia trimer has a triangular structure of C_{3h} symmetry; see Figure 1. We assigned two spectral features at 3444.6 and 3433.3 cm^{-1} in the spectral range of the ν_3 band to free N−H stretches. The calculations place the single A″ band at 3448 cm^{-1} close to the ν_3 band origin of the single NH_3 molecule. The other two bands at 3405 and 3448 cm^{-1} are of A′ and E″ symmetry, respectively, and have no infrared intensity. We were not able to detect any bands due to the free stretch vibrations of the trimers in the ν_1 range, in agreement with calculations that predict that the vibration at 3291 cm^{-1} of A′ type is not IR active.

The strong bands at about 3401 and 3316.5 cm^{-1} are assigned to the ν_3(E″) and ν_1(E′) bands, which are associated with a large amplitude of vibration of the hydrogen-bonded H atoms. The calculated IRIs, although in qualitative agreement with the experimental observations, are by a factor of 5−8 larger than the experimental results.

Similar to the case for the dimers, the ν_3 band in the trimers has two components that have an intensity ratio of about 4:3 and are split by about 3.8 cm^{-1}. The splitting of the E-type vibrations may indicate some deviation of the structure of the trimers from C_{3h} symmetry. We are somewhat puzzled by the similarity of the splitting of the ν_3 bands in trimers and dimers. In the last case the splitting could not be explained by the lifting of the degeneracy because of the low symmetry of the dimers. Moreover, no splitting could be identified in the spectra of the ν_1(E′) band of the trimers, which is consistent with the presence of a C_3 axis in the cluster.

According to calculations (cf. Table 2) the ammonia trimer $(NH_3)_3$ is an oblate symmetric top with rotational constants of $B_0 = 0.1723$ cm^{-1} and $C_0 = 0.0893$ cm^{-1}. In view of the small values of the rotational constants, no rotational structure is expected to appear in the spectra at the experimental laser line width of ∼0.3 cm^{-1}.

The spectra of the trimers show strong peaks in the range of the $2\nu_4$ band. In comparison, the overtone bands of dimers are very weak, similar to those in single ammonia molecules. However, in trimers both the $2\nu_4(l=2)$ and $2\nu_4(l=0)$ bands have IR intensities which are comparable to those in the fundamental bands.

The calculated anharmonic overtones for $2\nu_4$ in the trimer are 3215 and 3248 cm^{-1} (overtones of the fundamentals at 1626 and 1630 cm^{-1}) and 3154 and 3223 cm^{-1} (overtones of the fundamentals at 1581 and 1615 cm^{-1}). The calculated overtones are 30−100 cm^{-1} lower than the results of the measurements, as seen in Table 4. The observed large intensity of the overtone bands in the trimers is unexpected. Usually hydrogen bonding does not lead to any significant increase of the intensity of the

TABLE A1: Total (E_e) and Binding (ΔE_e) Energies for the Ammonia Clusters $(NH_3)_n$, $n = 1-4$[a]

	E_e, au		ΔE_e (ΔE_0), kcal/mol	
n	aug-cc-pVDZ	aug-cc-pVTZ	aug-cc-pVDZ	aug-cc-pVTZ
1 (C_{3v})	−56.404 889 87	−56.460 540 92		
2 (C_s)	−112.815 555 26	−112.926 318 60	−3.62 (−2.13)	−3.29 (−1.89)
3 (C_s)	−169.225 451 30		−6.77 (−4.31)	
3 (C_{3h})	−169.233 665 39	−169.399 110 46	−11.92 (−7.84)	−10.97 (−7.02)
4 (C_{3v})	−225.634 971 56		−9.67 (−6.44)	
4 (C_3)	−225.640 916 83		−13.40 (−8.82)	
4 (C_{4h})	−225.649 072 92		−18.52 (−12.60)	

[a] The binding energies are computed with respect to *n* gas-phase monomers. Zero-point corrected binding energies (ΔE_0) are shown in parentheses.

TABLE A2: Optimal Geometric Parameters at the Equilibrium and Vibrationally Averaged Geometries for the Ammonia Clusters $(NH_3)_n$, $n = 1-4$[a]

n		equilibrium geometry	vibrationally averaged geometry
1 (C_{3v})	R_f(N−H), Å	1.020	1.033
	α(H−N−H), deg	106.30	106.48
	δ[H−(N−H−H)], deg	112.97	113.33
2 (C_s)	R(N−N), Å	3.266	3.308
	R_b(N−H), Å	1.024	1.000
	R_f(N−H), Å	1.020 [5]	0.970, 0.967 [2], 0.955 [2]
	α(H−N−H), deg	106.78 [2], 106.27 [2], 106.23, 105.97	107.66 [2], 107.61, 105.94 [2], 105.44
	δ[H−(N−H−N)], deg	±109.80, ±123.49	±109.27, ±123.38
3 (C_{3h})	R(N−N), Å	3.183 [3]	3.231 [3]
	R_b(N−H), Å	1.027 [3]	1.014 [3]
	R_f(N−H), Å	1.020 [6]	0.988 [6]
	α(H−N−H), deg	106.79 [6], 105.91 [3]	107.08 [6], 105.55 [3]
	δ[H−(N−N−N)], deg	±101.59 [3], 0.00 [3]	±102.47 [3], 0.00 [3]
4 (C_{4h})	R(N−N), Å	3.175 [4]	
	R_b(N−H), Å	1.029 [4]	
	R_f(N−H), Å	1.020 [8]	
	α(H−N−H), deg	106.54 [8], 105.65 [4]	
	δ[H−(N−N−N)], deg	±113.35 [8], 0.00 [4]	

[a] All results shown are obtained at the MP2/aug-cc-pVDZ level of theory. Subscripts "f" and "b" denote the "free" and "hydrogen-bonded" N−H stretches, respectively. Numbers in brackets denote the total number of the internal coordinates which have the same value due to symmetry.

bending modes. Therefore, we concluded that the nominally $2\nu_4$ band must borrow intensity from the modes which are enhanced by the hydrogen bonding, i.e., ν_1 and ν_3 modes. The ν_1 mode is the most probable candidate for this intensity borrowing. In single molecules, the strength of the vibrational coupling of the ν_1 and $2\nu_4(l=0)$ bands amounts to 36.5 cm^{-1}.[14] Several factors contribute to the larger effect of the coupling in the clusters. The frequency difference between the ν_1 and $2\nu_4$ modes is expected to be smaller in clusters. The formation of the hydrogen bond leads to the decrease of the frequency of the ν_1 H-stretching mode, while at the same time the frequency of the ν_4 H-bending mode increases. Our anharmonic calculations at the MP2/aug-cc-pVDZ level yield frequencies of 3324, 3310, and 3293 cm^{-1} for the ν_1 mode of the monomer, dimer, and trimer clusters, respectively. The corresponding calculated frequencies of the ν_4 mode are 1604, 1618, and 1630 cm^{-1} (cf. Table 1). Therefore, calculations properly account for the decrease of the frequency difference between the $2\nu_4$ and the ν_1 modes. The formation of the trimer might, however, contribute to an additional increase of the coupling strength due to its rigid structure and nonlinearity of the hydrogen bond.

C. Tetramers. Figure 3 suggests that the increase of the cluster size results in a progressive lowering of the frequency of the ν_1 and ν_3 bands. However, this trend slows down in larger clusters. The shift of the ν_3 band of $(NH_3)_4$ relative to that for $(NH_3)_3$ amounts to only ~10 cm^{-1}. The ν_1 bands of the trimers and tetramers have essentially the same frequency and could not be resolved. In larger clusters of sizes of $n = 5-900$, which are not shown here, the centers of all bands gradually shift toward lower frequencies and their line widths increase.[52] Spectra of the large clusters having about 900 molecules are very similar to those obtained in ammonia crystals,[81] films,[82] and aerosol particles.[83] In the case of the ν_3 band about 60% of the shift from the frequency in single ammonia molecules to that in condensed phase occurs upon formation of trimers, followed by much slower convergence in the case of larger clusters. This may indicate that some structural change is accomplished upon the formation of trimers. The unit cell of the crystalline ammonia obtained with neutron scattering measurements[2] is shown in Figure 1. The triangular pattern of ammonia molecules in the crystal similar to that of an ammonia trimer can be easily recognized. Thus the ammonia trimer can be viewed as a primitive hydrogen-bonded unit of solid ammonia. The calculations indicate that the global minimum configuration of the $(NH_3)_4$ cluster corresponds to a structure of C_{4h} symmetry. The formation of the cyclic tetramer in He droplets must include an insertion of the NH_3 molecule in the preformed cyclic ammonia trimer. A similar process has been previously documented in the case of water clusters formed in He droplets.[84,85] It is not clear a priori if the same insertion takes place for ammonia clusters; however, the fact that hydrogen bonding in ammonia is weaker than in water will probably facilitate this process. Furthermore, the formation of the higher energy isomers of tetramer, such as the one of C_3 symmetry shown in Figure 1, could not be excluded. The observation of a rather sharp ν_1 band in the tetramer spectra is consistent with the formation of either the C_{4h} or C_3 symmetric isomer. The spectrum of the "tail" (or "3 + 1") isomer of $(NH_3)_4$[1] was found to have the ν_1 and ν_3 bands split by about 20−40 cm^{-1}. Because we did not observe such a splitting pattern in the spectra in Figures 2 and 3, the formation of this "tail" isomer of $(NH_3)_4$ in He droplets cannot be confirmed. The

TABLE A3: Effect of Vibrational Averaging on the Geometry and Spectroscopic Constants of NH_3 and Comparison with Experiment[a]

	MP2/aug-cc-pVDZ	MP2/aug-cc-pVTZ	experiment
$A_e = B_e$ (cm^{-1})	9.790 76	9.978 45	
C_e (cm^{-1})	6.274 27	6.336 12	
$A_0 = B_0$ (cm^{-1})	9.714 28	9.911 78	9.9440[b]
C_0 (cm^{-1})	6.156 15	6.221 51	6.1960[c]
D_J (cm^{-1})	$0.714\,815 \times 10^{-3}$	$0.744\,70 \times 10^{-3}$	0.811×10^{-3} [b]
D_{JK} (cm^{-1})	$-0.127\,05 \times 10^{-2}$	$-0.133\,07 \times 10^{-3}$	-0.151×10^{-2} [b]
D_K (cm^{-1})	$0.730\,36 \times 10^{-3}$	$0.763\,27 \times 10^{-3}$	
$\omega_1(A_1)$, cm^{-1} (I, km/mol)	3480 (4.6)	3503 (3.4)	
$\omega_2(A_1)$, cm^{-1} (I, km/mol)	1045 (131.0)	1037 (139.2)	
$\omega_3(E)$, cm^{-1} (I, km/mol)	3635 (5.1)	3650 (8.4)	
$\omega_4(E)$, cm^{-1} (I, km/mol)	1649 (13.3)	1669 (14.3)	
$\nu_1(A_1)$, cm^{-1}	3324	3360	3337[d]
$\nu_2(A_1)$, cm^{-1}	968	959	950[d]
$\nu_3(E)$, cm^{-1}	3459	3483	3444[d]
$\nu_4(E)$, cm^{-1}	1604	1621	1627[d]
ZPE(harmonic), cm^{-1}	7547.3	7589.0	
ZPE(fundamental), cm^{-1}	7209.3	7264.3	7214.5[d]
ZPE(anharmonic), cm^{-1}	7419.2	7463.9	
R_e(N−H), Å	1.020	1.012	
α_e(H−N−H), deg	106.30	106.77	
δ_e[H−(N−H−H)], deg	112.97	113.92	
R_0(N−H), Å	1.033	1.024	1.0156[b]
α_0(H−N−H), deg	106.48	106.96	107.17[b]
δ_0[H−(N−H−H)], deg	113.33	114.32	112.15[c]

[a] Subscript "e" denotes equilibrium whereas "0" indicates vibrationally averaged quantities. Symbols ω and ν indicate the harmonic and anharmonic frequencies, respectively. The intensities (in km/mol) of the harmonic frequencies are listed in parentheses. [b] Reference 76. [c] Reference 77. [d] Reference 78.

infrared spectra of the larger average size clusters ($n = 5-7$)[52] suggest that the ν_1 band has a width similar to that in $n = 3$ and 4. If the $(NH_3)_4$ clusters in He droplets adopt ring structures, it is reasonable to assume that the ring pattern will persist in pentamers, but the fifth molecule will occupy an asymmetric site on that ring. Indeed, a number of such structures have been proposed in recent calculations.[1] The calculated spectra of those clusters (see Figures 4 and 5 of ref 1) consist of a large number of lines of comparable intensity. This is in disconcert with the experimental results of this work, which show that the spectra of the tetramers and larger clusters are very similar. The structure of a pentamer having an arrangement of molecules similar to that in the crystal would consist of two triangular clusters, each having one common ammonia molecule.

D. Infrared Intensity. In ammonia clusters the formation of the hydrogen bonds results in the increase of the infrared intensity (IRI) which is shared between the ν_1, ν_3, and $2\nu_4$ bands. Therefore, it is useful to calculate the total IRIs of the enhanced bands per hydrogen bond in cluster (IRIB). In the dimers the IRIB amounts to (44 ± 9) km/mol, which is about 4 times larger than the IRI in a single ammonia molecule. In $(NH_3)_3$ and $(NH_3)_4$ the IRIB amounts to (45 ± 14) km/mol and (59 ± 30) km/mol, respectively, which, within the error bars, is the same as in the dimers. Here the assumption has been made that tetramers have four hydrogen bonds as in the C_{4h} structure in Figure 1. The C_3 isomer of the tetramer has three strong and three weak hydrogen bonds. These may contribute to the increase of the IRI in a different way, making IRIB ill-defined. Therefore, we will limit the following discussion to IRIB for dimers and trimers.

It is instructive to compare the obtained values of the IRIB with those in the ammonia crystal. From the absorption spectrum of the crystalline ammonia in the stretching region (3000−3600 cm^{-1}),[81] taking into account that each molecule is a triple donor and triple acceptor,[2] the IRIB could be obtained to be 51 km/mol. This result takes into account the common dielectric correction; i.e., the IRIB was multiplied by a factor of $9n/(n^2 + 2)^2$, where $n = 1.4$ is the refractive index of solid ammonia in the 3 μm spectral range.[81] It follows that the IRIB in ammonia dimers and trimers is the same as in the crystal within experimental error. This similarity of the IRIB in small ammonia clusters and in the crystal suggests that the binding in ammonia is dominated by mainly two-body interactions. This is consistent with the fact that the three-body term in ammonia trimer (11%)[86] is smaller than the corresponding one in the water trimer (17%).[73−75] Each ammonia molecule has a single lone-pair orbital. Consequently, even in small clusters the lone pair of an acceptor molecule is saturated. Our results suggest that the sharing of the single lone pair with additional donor molecules in the crystal does not lead to an increase of IRIB. This is in agreement with the weakness of the HB between ammonia molecules and indicates that the charge redistribution in ammonia molecules upon HB formation is small.

In the dimers the IRIB was calculated to be $A_2^{calc} = 139$ km/mol, as compared to the measured $A_2^{exp} = 44$ km/mol. For the trimers and tetramers the IRIs are calculated to be $A_3^{calc} = 518$ km/mol and $A_4^{calc} = 1100$ km/mol as compared to the measured $A_3^{exp} = 135$ km/mol and $A_4^{exp} = 238$ km/mol. Previous calcuations[1] produced values of the IRI similar to the results of the present study. These comparisons indicate that calculations overestimate infrared intensities in ammonia clusters by about a factor of 4. Moreover, the calculations yield values for the IRIB in clusters which are a factor of 4 larger than in the crystal, a result that is probably not realistic. The detailed origin of the overestimation of the IRI in the calculations is not clear at the moment. Some error is introduced by the use of the harmonic approximation and fixed cluster geometry.

V. Conclusions

In this work we studied the infrared spectra and intensities of the NH stretching vibrations of $(NH_3)_n$ clusters ($n = 2-4$) using the helium droplet isolation technique. The measured spectra exhibit well-resolved bands, which have been assigned

to the ν_1, ν_3, and $2\nu_4$ modes of the ammonia fragments in the clusters. The ν_1, ν_3, and $2\nu_4$ bands of clusters have been identified, and their infrared intensities have been obtained. In the dimers and trimers, weak bands exhibiting small shifts with respect to the band origins of the corresponding bands in single molecules have been assigned to free N−H stretches of the NH_3 molecules. Other bands, which have larger spectral shifts and a factor of about 4 larger intensities, were assigned to the modes having large amplitude vibrations along the respective hydrogen bonds. The assignment of the bands is facilitated by the results of first principles electronic structure calculations for the anharmonic spectra of the clusters. In general, there is very good agreement between the experimentally measured band origins and the calculated anharmonic vibrational frequencies. Typical differences between the calculated and experimentally measured frequencies amount to less than 20 cm^{-1} (or 0.6%) for the strong NH stretching fundamental bands.

The dimerization of ammonia leads to an increase of the infrared intensity by a factor of about 4, caused by formation of the hydrogen bond. In the trimer the infrared intensity per hydrogen bond is close to that of the dimer. This is consistent with the relatively small magnitude (11%) of the three-body interactions, in agreement with the results of our calculations. In the trimers and tetramers the intensity of the $2\nu_4$ overtone band increases by a factor of about 10 relative to that in the monomer and dimer, and is comparable to the intensity of the ν_1 and ν_3 fundamental bands. This indicates the onset of the strong coupling of the $2\nu_4$ and ν_1 modes in trimers and larger clusters. The comparison of the calculated and measured infrared intensities indicates that the harmonic calculations overestimate infrared intensities in ammonia clusters by about a factor of 4. One possible explanation for this discrepancy rests with the possibility of strong coupling to other modes as a result of the intermolecular interactions. Models that allow for the coupling of bond modes in an approximate fashion, such as the harmonically coupled anharmonic oscillator (HCAO),[87−89] have been previously used to successfully predict the fundamental and overtone intensities of hydrogen-bonded molecular systems.[90−93] The ability of those models to reproduce the experimentally observed IR intensities for ammonia clusters will be investigated in future studies.

Acknowledgment. B.G.S. thanks the University of Southern California for financial support. We acknowledge the Donors of the American Chemical Society, Petroleum Research Fund, and the National Science Foundation (Grant CHE 0513163) for partial support. Part of this work was performed under the auspices of the Division of Chemical Sciences, Office of Basic Energy Sciences, Geosciences and Biosciences, U.S. Department of Energy under Contract No. DE-AC06-76RLO 1830 with Battelle Memorial Institute, which operates the Pacific Northwest National Laboratory. Computer resources at the National Energy Research Scientific Computer Center (NERSC) were provided by the Division of Chemical Sciences, U.S. Department of Energy.

References and Notes

(1) Janeiro-Barral, P. E.; Mella, M. *J. Phys. Chem. A* **2006**, *110*, 11244.
(2) Hewat, A. W.; Riekel, C. *Acta Crystallogr., Sect. A* **1979**, *35*, 569.
(3) Xantheas, S. S. *J. Chem. Phys.* **1996**, *104*, 8821.
(4) Halkier, A.; Jorgensem, P.; Christiansen, O.; Nielsen, I. B. M.; Helgaker, T. *Theor. Chem. Acc.* **1997**, *97*, 150.
(5) Belov, S. P.; Gershstein, L. I.; Krupnov, A. F.; Maslovskij, A. V.; Urban, S.; Spirko, V.; Papousek, D. *J. Mol. Spectrosc.* **1980**, *84*, 288.
(6) Belov, S. P.; Urban, S.; Winnewisser, G. *J. Mol. Spectrosc.* **1998**, *189*, 1.
(7) Marshall, M. D.; Izgi, K. C.; Muenter, J. S. *J. Chem. Phys.* **1997**, *107*, 1037.
(8) Ozier, I.; Meerts, W. L. *J. Chem. Phys.* **1987**, *86*, 2548.
(9) Sasada, H.; Endo, Y.; Hirota, E.; Poynter, R. L.; Margolis, J. S. *J. Mol. Spectrosc.* **1992**, *151*, 33.
(10) Sasada, H.; Hasegawa, Y.; Amano, T.; Shimizu, T. *J. Mol. Spectrosc.* **1982**, *96*, 106.
(11) Tanaka, K.; Endo, Y.; Hirota, E. *Chem. Phys. Lett.* **1988**, *146*, 165.
(12) Urban, S.; Papousek, D.; Belov, S. P.; Krupnov, A. F.; Tretyakov, M. Y.; Yamada, K.; Winnewisser, G. *J. Mol. Spectrosc.* **1983**, *101*, 16.
(13) Urban, S.; Spirko, V.; Papousek, D.; Kauppinen, J.; Belov, S. P.; Gershtein, L. I.; Krupnov, A. F. *J. Mol. Spectrosc.* **1981**, *88*, 274.
(14) Kleiner, I.; Brown, L. R.; Tarrago, G.; Kuo, Q.-L.; Picque', N.; Guelachvili, G.; Dana, V.; Mandin, J.-Y. *J. Mol. Spectrosc.* **1999**, *193*, 46.
(15) Cotti, G.; Linnartz, H.; Meerts, W. L.; Avoird, A. v. d.; Olthof, E. H. T. *J. Chem. Phys.* **1996**, *104*, 3898.
(16) Fraser, G. T.; Nelson, D. D.; Charo, A.; Klemperer, W. *J. Chem. Phys.* **1985**, *82*, 2535.
(17) Havenith, M.; Cohen, R. C.; Busarow, K. L.; Gwo, D. H.; Lee, Y. T.; Saykally, R. J. *J. Chem. Phys.* **1991**, *94*, 4776.
(18) Havenith, M.; Linnartz, H.; Zwart, E.; Kips, A.; Termeulen, J. J.; Meerts, W. L. *Chem. Phys. Lett.* **1992**, *193*, 261.
(19) Linnartz, H.; Kips, A.; Meerts, W. L.; Havenith, M. *J. Chem. Phys.* **1993**, *99*, 2449.
(20) Linnartz, H.; Meerts, W. L.; Havenith, M. *Chem. Phys.* **1995**, *193*, 327.
(21) Loeser, J. G.; Schmuttenmaer, C. A.; Cohen, R. C.; Elrod, M. J.; Steyert, D. W.; Saykally, R. J.; Bumgarner, R. E.; Blake, G. A. *J. Chem. Phys.* **1992**, *97*, 4727.
(22) Nelson, D. D.; Fraser, G. T.; Klemperer, W. *J. Chem. Phys.* **1985**, *83*, 6201.
(23) Nelson, D. D.; Fraser, G. T.; Klemperer, W. *Science* **1987**, *238*, 1670.
(24) Nelson, D. D.; Klemperer, W.; Fraser, G. T.; Lovas, F. J.; Suenram, R. D. *J. Chem. Phys.* **1987**, *87*, 6364.
(25) Olthof, E. H. T.; Vanderavoird, A.; Wormer, P. E. S. *J. Chem. Phys.* **1994**, *101*, 8430.
(26) Olthof, E. H. T.; Vanderavoird, A.; Wormer, P. E. S. *THEOCHEM (J. Mol. Struct.)* **1994**, *113*, 201.
(27) Olthof, E. H. T.; Vanderavoird, A.; Wormer, P. E. S.; Loeser, J. G.; Saykally, R. J. *J. Chem. Phys.* **1994**, *101*, 8443.
(28) Van der Avoird, A.; Olthof, E. H. T.; Wormer, P. E. S. *Faraday Discuss.* **1994**, *97*, 43.
(29) Beu, T. A.; Buck, U. *J. Chem. Phys.* **2001**, *114*, 7848.
(30) Kulkarni, S. A.; Pathak, R. K. *Chem. Phys. Lett.* **2001**, *336*, 278.
(31) Yeo, G. A.; Ford, T. A. *Spectrochim. Acta, Part A* **1994**, *50*, 5.
(32) Greer, J. C.; Ahlrichs, R.; Hertel, I. V. *Chem. Phys.* **1989**, *133*, 191.
(33) Dykstra, C. E.; Andrews, L. *J. Chem. Phys.* **1990**, *92*, 6043.
(34) Szczesniak, M. M.; Kendall, R. A.; Chalasinski, G. *J. Chem. Phys.* **1991**, *95*, 5169.
(35) Beu, T. A.; Buck, U. *J. Chem. Phys.* **2001**, *114*, 7853.
(36) Yeo, G. A.; Ford, T. A. *Struct. Chem.* **1992**, *3*, 75.
(37) Xantheas, S. S.; Dunning, T. H. *J. Chem. Phys.* **1993**, *98*, 8037.
(38) Xantheas, S. S. *J. Chem. Phys.* **1994**, *100*, 7523.
(39) Xantheas, S. S. *Chem. Rev.* **2000**, *258*, 225.
(40) Heijmen, B.; Bizzarri, A.; Stolte, S.; Reuss, J. *Chem. Phys.* **1988**, *126*, 201.
(41) Howard, M. J.; Burdenski, S.; Giese, C. F.; Gentry, W. R. *J. Chem. Phys.* **1984**, *80*, 4137.
(42) Huisken, F.; Pertsch, T. *Chem. Phys.* **1988**, *126*, 213.
(43) Snels, M.; Fantoni, R.; Sanders, R.; Meerts, W. L. *Chem. Phys.* **1987**, *115*, 79.
(44) Behrens, M.; Buck, U.; Frochtenicht, R.; Hartmann, M.; Havenith, M. *J. Chem. Phys.* **1997**, *107*, 7179.
(45) Odutola, J. A.; Dyke, T. R.; Howard, B. J.; Muenter, J. S. *J. Chem. Phys.* **1979**, *70*, 4884.
(46) Pimentel, G. C.; Bulanin, M. O.; Thiel, M. V. *J. Chem. Phys.* **1962**, *36*, 500.
(47) Suzer, S.; Andrews, L. *J. Chem. Phys.* **1987**, *87*, 5131.
(48) Steinbach, C.; Buck, U.; Beu, T. A. *J. Chem. Phys.* **2006**, *125*, 133403.
(49) Liu, Y. Q.; Suhm, M. A.; Botschwina, P. *Phys. Chem. Chem. Phys.* **2004**, *6*, 4642.
(50) Barth, H. D.; Huisken, F. *J. Chem. Phys.* **1987**, *87*, 2549.
(51) Slipchenko, M.; Kuyanov, K.; Sartakov, B.; Vilesov, A. F. *J. Chem. Phys.* **2006**, *124*, 241101.
(52) Slipchenko, M.; Vilesov, A. To be published, **2007**.
(53) Toennies, J. P.; Vilesov, A. F. *Angew. Chem., Int. Ed.* **2004**, *43*, 2622.
(54) Toennies, J. P.; Vilesov, A. F. *Annu. Rev. Phys. Chem.* **1998**, *49*, 1.

(55) Callegari, C.; Lehmann, K. K.; Schmied, R.; Scoles, G. *J. Chem. Phys.* **2001**, *115*, 10090.
(56) Hartmann, M.; Miller, R. E.; Toennies, J. P.; Vilesov, A. F. *Science* **1996**, *272*, 1631.
(57) Choi, M. Y.; Douberly, G. E.; Falconer, T. M.; Lewis, W. K.; Lindsay, C. M.; Merritt, J. M.; Stiles, P. L.; Miller, R. E. *Int. Rev. Phys. Chem.* **2006**, *25*, 15.
(58) Hartmann, M.; Miller, R. E.; Toennies, J. P.; Vilesov, A. *Phys. Rev. Lett.* **1995**, *75*, 1566.
(59) Dunning, T. H. *J. Chem. Phys.* **1989**, *90*, 1007.
(60) Kendall, R. A.; Dunning, T. H.; Harrison, R. J. *J. Chem. Phys.* **1992**, *96*, 6796.
(61) Clabo, D. A.; Allen, W. D.; Remington, R. B.; Yamaguchi, Y.; Schaefer, H. F. *Chem. Phys.* **1988**, *123*, 187.
(62) Allen, W. D.; Yamaguchi, Y.; Csaszar, A. G.; Clabo, D. A.; Remington, R. B.; Schaefer, H. F. *Chem. Phys.* **1990**, *145*, 427.
(63) Miller, W. H.; Hernandez, R.; Handy, N. C.; Jayatilaka, D.; Willetts, A. *Chem. Phys. Lett.* **1990**, *172*, 62.
(64) Barone, V. *J. Chem. Phys.* **2004**, *120*, 3059.
(65) Barone, V.; Carbonniere, P.; Pouchan, C. *J. Chem. Phys.* **2005**, *122*.
(66) Shneider, W.; Thiel, W. *Chem. Phys. Lett.* **1989**, *157*, 367.
(67) Barone, V. *J. Chem. Phys.* **1994**, *101*, 10666.
(68) Barone, V.; Adamo, C.; Minichino, C. *THEOCHEM (J. Mol. Struct.)* **1995**, *330*, 325.
(69) Minichino, C.; Barone, V. *J. Chem. Phys.* **1994**, *100*, 3717.
(70) Xantheas, S. S. *Int. Rev. Phys. Chem.* **2006**, *25*, 719.
(71) Frisch, M. J.; Trucks, G. W.; Schlegel, H. B.; Scuseria, G. E.; Robb, M. A.; Cheeseman, J. R.; Zakrzewski, V. G.; Montgomery, J. A., Jr.; Stratmann, R. E.; Burant, J. C.; Dapprich, S.; Millam, J. M.; Daniels, A. D.; Kudin, K. N.; Strain, M. C.; Farkas, O.; Tomasi, J.; Barone, V.; Cossi, M.; Cammi, R.; Mennucci, B.; Pomelli, C.; Adamo, C.; Clifford, S.; Ochterski, J.; Petersson, G. A.; Ayala, P. Y.; Cui, Q.; Morokuma, K.; Malick, D. K.; Rabuck, A. D.; Raghavachari, K.; Foresman, J. B.; Cioslowski, J.; Ortiz, J. V.; Baboul, A. G.; Stefanov, B. B.; Liu, G.; Liashenko, A.; Piskorz, P.; Komaromi, I.; Gomperts, R.; Martin, R. L.; Fox, D. J.; Keith, T.; Al-Laham, M. A.; Peng, C. Y.; Nanayakkara, A.; Challacombe, M.; Gill, P. M. W.; Johnson, B.; Chen, W.; Wong, M. W.; Andres, J. L.; Gonzalez, C.; Head-Gordon, M.; Replogle, E. S.; Pople, J. A. *Gaussian 98*, revision A.9; Gaussian, Inc.: Pittsburgh, PA, 1998.
(72) Frisch, M. J.; Trucks, G. W.; Schlegel, H. B.; Scuseria, G. E.; Robb, M. A.; Cheeseman, J. R.; Montgomery, J. A., Jr.; Vreven, T.; Kudin, K. N.; Burant, J. C.; Millam, J. M.; Iyengar, S. S.; Tomasi, J.; Barone, V.; Mennucci, B.; Cossi, M.; Scalmani, G.; Rega, N.; Petersson, G. A.; Nakatsuji, H.; Hada, M.; Ehara, M.; Toyota, K.; Fukuda, R.; Hasegawa, J.; Ishida, M.; Nakajima, T.; Honda, Y.; Kitao, O.; Nakai, H.; Klene, M.; Li, X.; Knox, J. E.; Hratchian, H. P.; Cross, J. B.; Bakken, V.; Adamo, C.; Jaramillo, J.; Gomperts, R.; Stratmann, R. E.; Yazyev, O.; Austin, A. J.; Cammi, R.; Pomelli, C.; Ochterski, J. W.; Ayala, P. Y.; Morokuma, K.; Voth, G. A.; Salvador, P.; Dannenberg, J. J.; Zakrzewski, V. G.; Dapprich, S.; Daniels, A. D.; Strain, M. C.; Farkas, O.; Malick, D. K.; Rabuck, A. D.; Raghavachari, K.; Foresman, J. B.; Ortiz, J. V.; Cui, Q.; Baboul, A. G.; Clifford, S.; Cioslowski, J.; Stefanov, B. B.; Liu, G.; Liashenko, A.; Piskorz, P.; Komaromi, I.; Martin, R. L.; Fox, D. J.; Keith, T.; Al-Laham, M. A.; Peng, C. Y.; Nanayakkara, A.; Challacombe, M.; Gill, P. M. W.; Johnson, B.; Chen, W.; Wong, M. W.; Gonzalez, C.; Pople, J. A. *Gaussian 03*, revision C.02; Gaussian, Inc.: Wallingford CT, 2004.
(73) Xantheas, S. S. *Philos. Mag. B* **1996**, *73*, 107.
(74) Xantheas, S. S. *Chem. Phys.* **2000**, *258*, 225.
(75) Xantheas, S. S.; Dunning, T. H. *J. Chem. Phys.* **1993**, *99*, 8774.
(76) Mould, H. M.; W. C. P. a. G. R. W. *Spectrochim. Acta* **1959**, *15*, 313.
(77) Herzberg, G. *Electronic spectra and electronic structure of polyatomic molecules*; Van Nostrand: New York, 1966.
(78) Shimanouchi, T. *Tables of Molecular Vibrational Frequencies Consolidated*; National Bureau of Standards: Washington, DC, 1972; Vol. 1.
(79) Slipchenko, M. N.; Vilesov, A. F. *Chem. Phys. Lett.* **2005**, *412*, 176.
(80) Stiles, P. L.; Nauta, K.; Miller, R. E. *Phys. Rev. Lett.* **2003**, *90*, 135301.
(81) Sill, G.; Fink, U.; Ferraro, J. R. *J. Opt. Soc. Am.* **1980**, *70*, 724.
(82) Holt, J. S.; Sadoskas, D.; Pursell, C. J. *J. Chem. Phys.* **2004**, *120*, 7153.
(83) Jetzki, M.; Bonnamy, A.; Signorell, R. *J. Chem. Phys.* **2004**, *120*, 11775.
(84) Nauta, K.; Miller, R. E. *Science* **2000**, *287*, 293.
(85) Burnham, C. J.; Xantheas, S. S.; Miller, M. A.; Applegate, B. E.; Miller, R. E. *J. Chem. Phys.* **2002**, *117*, 1109.
(86) Xantheas, S. S. Unpublished results.
(87) Watson, I. A.; Henry, B. R.; Ross, I. G. *Spectrochim. Acta, Part A* **1981**, *37*, 857.
(88) Mortensen, O. S.; Henry, B. R.; Mohammadi, M. A. *J. Chem. Phys.* **1981**, *75*, 4800.
(89) Child, M. S.; Lawton, R. T. *Faraday Discuss. Chem. Soc.* **1981**, *71*, 273.
(90) Schofield, D. P.; Land, J. R.; Kjaergaard, H. G. *J. Phys. Chem. A* **2007**, *111*, 567.
(91) Howard, D. L.; Kjaergaard, H. G. *J. Phys. Chem. A* **2006**, *110*, 10245.
(92) Schofield, D. P.; Kjaergaard, H. G. *Phys. Chem. Chem. Phys.* **2003**, *5*, 3100.
(93) Cooper, P. D.; Kjaergaard, H. G.; Langford, V. S.; McKinley, A. J.; Quickenden, T. I.; Schofield, D. P. *J. Am. Chem. Soc.* **2003**, *125*, 6048.